Am J Cancer Res 2023;13(3):992-1003
www.ajcr.us /ISSN:2156-6976/ajcr0144677

Original Article

PTPMT1 regulates mitochondrial death through the SLC25A6-NDUFS2 axis in pancreatic cancer cells

Peng-Peng Ding[1*], Xiao-Dong Huang[2*], Lei Shen[3*], Li Du[4], Xiao-Chen Cheng[4], Yu-Xin Lu[4], Hong Liu[1], Dong-Dong Lin[2], Feng-Jun Xiao[4]

[1]Department of Gastroenterology, Beijing Shijitan Hospital of Capital Medical University, Beijing 100038, P. R. China; [2]Department of General Surgery, Xuanwu Hospital Capital Medical University, Beijing 100053, P. R. China; [3]Department of Gastroenterology, The First Medical Center of PLA General Hospital, Beijing 100853, P. R. China; [4]Department of Experimental Hematology and Biochemistry, Beijing Institute of Radiation Medicine, Beijing 100850, P. R. China. [*]Co-first authors.

Received June 10, 2022; Accepted December 27, 2022; Epub March 15, 2023; Published March 30, 2023

Abstract: Pancreatic ductal adenocarcinoma is a highly malignant cancer with poor prognosis, for which effective therapeutic strategies are urgently needed. The dual-specificity phosphatase PTPMT1 is localized in mitochondria and highly expressed in various cancers. Here, we investigated the function of PTPMT1 in pancreatic ductal adenocarcinoma. We inhibited its expression in pancreatic cancer cell lines using siRNAs or the specific PTPMT1 inhibitor alexidine dihydrochloride and observed that PTPMT1 silencing in pancreatic cancer cell lines drastically reduced cell viability, caused mitochondrial damage, and impaired mitochondrial function. Co-immunoprecipitation analysis demonstrated that PTPMT1 could interact with SLC25A6 and NDUFS2, indicating that it may modulate mitochondrial function via the SLC25A6-NDUFS2 axis. Collecively, our data highlight PTPMT1 as an important factor in pancreatic ductal adenocarcinoma and a potential therapeutic target.

Keywords: Pancreatic ductal adenocarcinoma, PTPMT1, SLC25A6, alexidine dihydrochloride

Introduction

Pancreatic ductal adenocarcinoma (PDAC) is the most frequently occurring type of pancreatic cancer whose global burden has doubled in the past few decades [1]. The prognosis of PDAC is dismal, with the 5-year survival rate at around 10% and a substantial chance of recurrence even following early-stage surgical resection [2]. Therefore, effective strategies for the treatment of PDAC are urgently needed.

PTPMT1 (Protein Tyrosine Phosphatase Mitochondrial 1) is a dual-specificity protein tyrosine phosphatase [3]. Investigations have shown that the glycerophospholipid PGP is a PTPMT1 target and regulates cardiac phospholipid biosynthesis and mitochondrial function [4, 5]. Downregulation of PTPMT1 in pancreatic beta cells increases cellular ATP levels and insulin production [6]. It has been reported that systemic deletion of PTPMT1 in mice results in embryonic lethality, supporting PTPMT1's vital role during development [7]. PTPMT1 has also been shown to regulate cell cycle and differentiation in hematopoietic stem cells by modulating mitochondrial metabolism [8]. The Ser/Arg-rich splicing factor 1 (SRSF1) can influence tumorigenesis and development by regulating PTPMT1 alternative splicing [9]. A genome-wide CRISPR-Cas9 knockout screen has found that PTPMT1 is critical for hypoxic survival of liver cancer during cardiolipin synthesis, and that PTPMT1 silencing prevents cardiolipin maturation, which in turn leads to ROS accumulation during hypoxia. PTPMT1 exhibited a high sensitivity to the PTPMT1 inhibitor alexidine dihydrochloride (AD), particularly under hypoxic circumstances [10, 11]. These findings have uncovered the protective role of PTPMT1 in hypoxia survival and cancer development. PTPMT1 inhibition results in cancer cell death, likely caused by metabolic crisis [12]. We showed previously that PTPMT1 could modulate the proliferation, survival, as well as glucose metabolism of erythroleukemia cells by inducing HIF2a expres-

sion, and that PTPMT1 knockout caused mitochondrial dysfunction [13]. Further studies have found that PTPMT1 inhibits ferroptosis in PANC-1 cells by inhibiting ACSL4 expression and upregulating SLC7A11 [14]. Although these data have demonstrated the importance of PTPMT1 to cancer cell survival, the precise mechanisms remain unclear. Here, we investigated the mechanisms by which PTPMT1 regulates mitochondrial death in two PDAC cell lines (PANC-1 and MIA-PACA-II) and proved its therapeutic value in the treatment of PDAC.

Materials and methods

Cell culture

The human PDAC cell lines PANC-1 and MIA-PACA-II cell were cultured in DMEM (#1196-5084, Gibco) supplemented with 10% fetal bovine serum (FBS) along with 100 U/ml penicillin-streptomycin (#10378016, Gibco) under 37°C and 5% CO_2 conditions. PANC05.04 cells were cultured in F12k media (#21127022, Gibco) supplemented with 10% FBS. ASPC-1 cells were cultured in RPMI 1640 media (#11875101, Gibco) supplemented with 10% FBS.

Lentivirus and siRNA transfection

Lentivirus infection: pLKO.1-*PTPMT1*-shRNA along with control lentiviral vectors were purchased from Sigma. The puromycin-resistance gene was replaced with RFP sequences to create the lentiviral vector pLKO.1-*PTPMT1*-shRNA (RFP). Lentiviral particles were generated by co-transfecting HEK293T cells with lentiviral vectors and packaging plasmids (psPAX2 and pMD2.G). We collected viral particles from supernatants, which were filtered and concentrated using PEG-it. Cells were infected with lentiviruses at a multiplicity of infection (MOI) of 10, as determined by viral titering. Infection efficiency was evaluated based on RFP expression levels as measured by a flow cytometer (BD, Fortessa).

siRNA transfection: siRNAs (Sangon Biotech, China) were transfected into cells using RNAiMAX (#13778 075, Gibco) and Opti-MEM (#37985070, Gibco) based on the manufacturer's instructions. The siRNA sequences are shown in Supplementary Table 2. Knockdown efficiency was assayed by western blotting.

Real-time PCR

The mRNA levels of *PTPMT1, SLC25A6*, and *NDUFS2* in pancreatic cancer cells were determined using RT-qPCR analysis. Total RNA was extracted from cultured cells and 1 mg of total RNA was converted to cDNA using the Revert Aid RT reverse transcription kit (#K1691, Thermo Fisher Scientific). Real-time PCR was done using the SYBR-green premix (#RR600/601, Takara) on a Studio Q3 real-time PCR system (Life Technologies). Relative gene expression was determined using the comparative Ct approach and normalized to β-actin. Sequences of the primers are given in Supplementary Table 1.

Western blot analysis

The NP40 (#AR0107, Boster) lysis buffer containing proteinase inhibitor and PMSF was used to lyse cells for 30 min. Equal protein amounts were resolved by SDS-PAGE (12%) and blotted onto PVDF membranes. The membranes were then blocked for one hour and incubated with primary antibodies against SLC25A6 (#14841-1-AP, Proteintech), PTPMT1 (#822944, ZEN BIO), or NDUFS2 (#R27071, ZEN BIO), followed by incubation with appropriate HRP-linked secondary antibodies (#111-035-003, Jackson) and visualization using enhanced ECL chemiluminescence (#WBKLS0100, Millipore).

CCK8 cell proliferation assay

Cell viability was assessed using the CCK8 assay kit as described by the manufacturer (bimake, American). Briefly, 2×10^4/mL cells were seeded in 96-well plates and treated accordingly. Then, 10 μl of the CCK-8 solution was added into each well and the cells were incubated for two hours before absorbance reading at 450 nm on a microplate reader (i3, Molecular Devices).

Mitochondrial membrane potential assay

Mitochondrial viability was assessed using the JC-1 detection kit as described by the manufacturer (Beyotime Biotechnology, China), which quantifies mitochondrial membrane potential (DWm) via measuring fluorescence intensities of red-shifted monomer aggregates along with green-shifted JC-1 monomers. In functional mitochondria with high DWm, the formed JC-1 aggregates are red-shifted, while JC-1 mono-

mers are green-shifted in damaged mitochondria with reduced DWm. The fluorescence of green-shifted JC-1 monomers linearly correlates with reduced DWm. Cells were rinsed thrice in 1 × PBS buffer and a JC-1 fluorescent probe was prepared. After staining at 37°C for 30 min, red and green fluorescence was analyzed using a flow cytometer (BD, Fortessa).

Colony formation assay

For colony formation analysis, 1,000-1,500 cells per well were plated in six-well plates and allowed to grow for 14 days after the indicated treatments. We then fixed the cells with absolute ethyl alcohol, and stained the cells with 5% crystal violet.

Analysis of mitochondrial activity

Cells were plated on poly-l-lysine-coated glass coverslips and treated with AD. Afterwards, we stained the cells with 100 nM MitoTracker Deep Green staining solution in the dark for 30 min to visualize mitochondria, followed by confocal imaging (ZEISS, Germany). Mitochondrial fluorescence intensity was quantified using ImageJ (version 1.48).

Co-immunoprecipitation

Total proteins were extracted from PANC-1 cells using NP40 lysis buffer and lysates were precleared with anti-species-specific IgG beads. Supernatants were then incubated with anti-SLC25A6 (#14841-1-AP, Proteintech), anti-PTPMT1 (#822944, ZEN BIO), or anti-NDUFS2 (#R27071, ZEN BIO) antibodies for one hour at 4°C. Next, we added protein G agarose beads and rotated the samples overnight at 4°C. Co-immunoprecipitated targets were then evaluated using western blotting.

Clinical samples

Between June 2015 and September 2017, fifty pairs of PDAC tissues along with neighboring non-tumorous pancreatic tissues were acquired from the Department of Hepato-Pancreato-Biliary Surgery, First Medical Center of Chinese PLA General Hospital. We obtained informed consent from each subject. The Chinese PLA General Hospital's Institutional Review Committee granted permission for the research. All pathology results were validated by two pathologists from the Chinese PLA General Hospital's pathology department. Supplementary Table 2 provides a summary of the clinical data along with baseline features of individuals with PDAC. The American Joint Committee on Cancer standards for grading and staging pancreatic cancer were followed.

Immunohistochemistry (IHC)

IHC analyses were done by the Servicebio company (Wuhan, China) using primary antibodies against SLC25A6, PTPMT1, and NDUFS2 at 1:100. The expression levels of SLC25A6, PTPMT1, and NDUFS2 were assessed using the H score approach (semi-quantitative analyses) through multiplying the percentage of positive cells (0-5%: 0 points, 6-25%: 1 points, 26-50%: 2 points, 51-75%: 3 points, >75%: 4 points) and the staining intensity (1, 2 and 3 indicating low, medium and strong intensity), respectively. A median H score of ≤4 indicates low expression, a median H score of >5 indicates high expression. The results were examined by two experienced pathologists at the PLA general hospital and reported as average H scores.

Statistical analysis

Data analyses were carried out using SPSS 21.0 (IBM Corp., USA) as well as GraphPad Prism 5 (GraphPad Software, CA). All results were from three independent experiments. Normally distributed data were given as mean ± SEM. Statistical comparisons between groups were assessed using the Student's T test (two-tailed) and ANOVA analysis. Statistical significance was denoted by $P<0.05$.

Results

PTPMT1 silencing inhibits cell proliferation and affects mitochondrial function

We first tested the expression level of PTPMT1 in different pancreatic cell lines (PANC05.04, PANC-1, MIA-CAPA-II, and ASPC-1). The results showed that the expression of PTPMT1 was higher in PANC-1 and MIA-PACA-II cells (**Figure 1A**). These two cell lines were therefore used further to confirm our main conclusions. Two different siRNAs were used to inhibit PTPMT1 in PANC-1 (**Figure 1B**, **1C**, ***P<0.001) and MIA-PACA-II (**Figure 1D**, **1E**, ***P<0.001) cells,

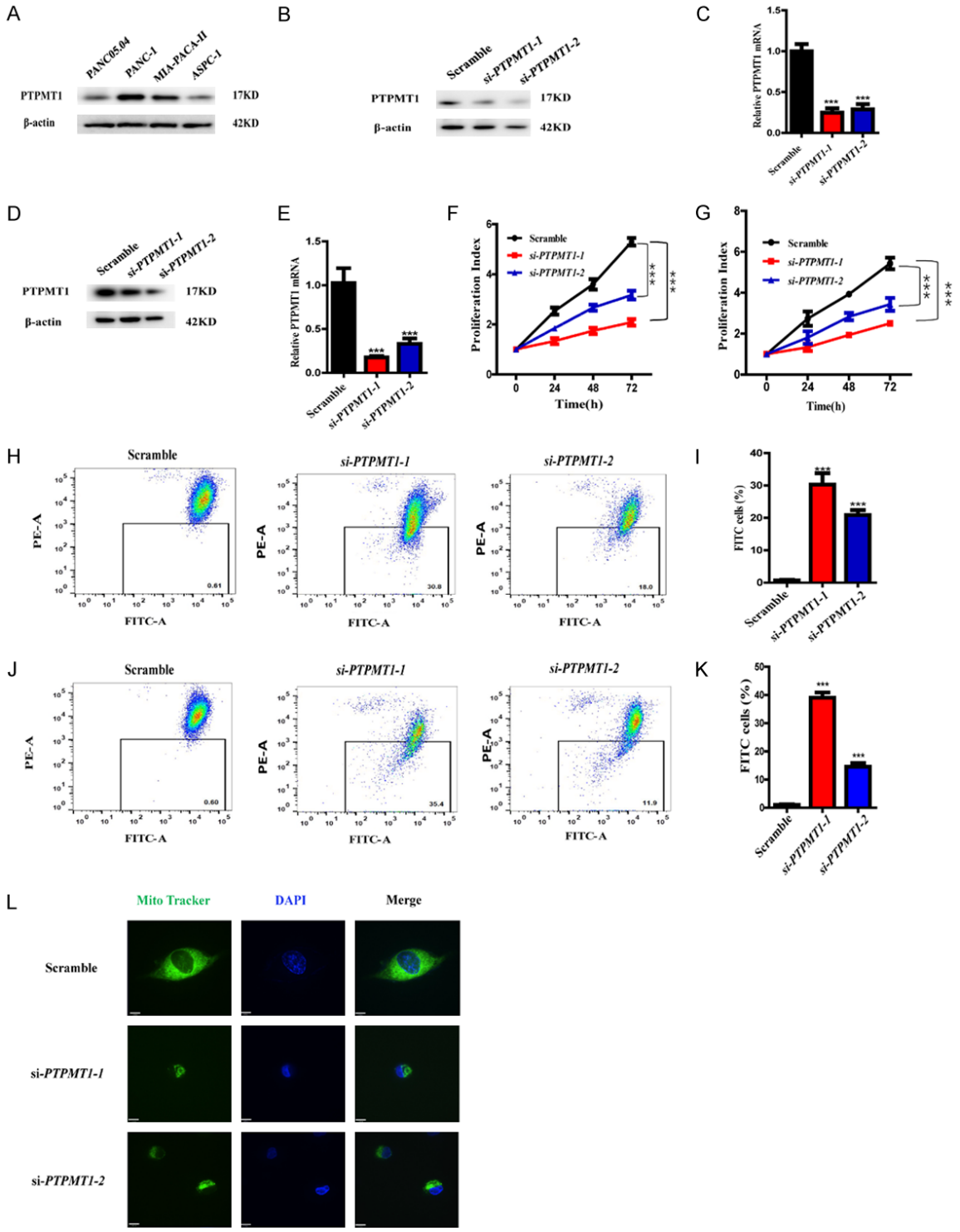

Figure 1. PTPMT1 silencing inhibits cell proliferation and affects mitochondrial function. (A) PTPMT1 protein levels were detected in different pancreatic cancer cell lines. (B) PTPMT1 protein levels in PANC-1 cells transfected with si-*PTPMT1* was analyzed using western blotting. (C) The mRNA levels of PTPMT1-silenced PANC-1 cells were analyzed by RT-qPCR. (D) PTPMT1 protein levels in MIA-PACA-II cells transfected with si-*PTPMT1* were analyzed by using western blotting. (E) The mRNA levels of PTPMT1-silecned MIA-PACA-II cells were analyzed by RT-qPCR. (F) Proliferation of PANC-1 cells silenced for PTPMT1 or expressing scrambled siRNAs was assessed by CCK8 analysis. (G) Proliferation of MIA-PACA-II cells silenced for PTPMT1 or expressing scrambled siRNAs was assessed by CCK8 analysis. (H) FACS analysis of the rate of mitochondrial damage in PTPMT1-silenced and scramble-transfected PANC-1 cells. (I)

Quantification of the proportion of mitochondria-damaged PANC-1 cells. (J) FACS analysis of the rate of mitochondrial damage in PTPMT1-silenced and scramble-transfected MIA-PACA-II cells. (K) Quantification of the proportion of mitochondria-damaged MIA-PACA-II cells. (L) Confocal analysis of mitochondrial morphology in PTPMT1-silenced and scramble-transfectedPANC-1 cells (Scale bar: 10 μm; Magnification: 600 ×). Data are given as mean ± SD of three independent experiments (C, E-G, I, K). ***P<0.001 (two-tailed t-test, C, E-G, I, K). β-actin (A, B, D): loading control. Data represent at least two independent experiments (A, B, D, F, G).

and the result showed that PTPMT1 was downregulated at both protein and mRNA levels. Next, we examined the effect of PTPMT1 on mitochondrial function, as well as cell survival, proliferation, and apoptosis in PANC-1 and MIA-PACA-II cells transinfected with *PTPMT1*-siRNA. This analysis showed that compared to cells transfected with the control siRNA, *PTPMT1* silencing dramatically inhibited cell growth in PANC-1 cells (**Figure 1F**, ***P<0.001) and MIA-PACA-II cells (**Figure 1G**, ***P<0.001). *PTPMT1* silencing also significantly increased the rate of JC-1 transition from red to green fluorescence and reduced mitochondrial membrane potential in both PANC-1 cells (**Figure 1H**, **1I**) and MIA-PACA-II cells (**Figure 1J**, **1K**). Moreover, confocal analysis revealed that the mitochondria in the cytoplasm of *PTPMT1*-silenced cells were considerably shorter and fewer than those in control cells (**Figure 1L**).

The PTPMT1 inhibitor Alexidine dihydrochloride suppresses the viability of PANC-1 cells and promotes apoptosis

Alexidine dihydrochloride (AD) is a specific PTPMT1 inhibitor. Colony formation assessment of the effect of AD on PANC-1 cell growth found that AD could drastically retard cell growth (**Figure 2A**, P<0.001) and reduce PANC-1 cell viability, in a dose-dependent manner (**Figure 2B**). Expression of PTPMT1 was significantly suppressed in PANC-1 cells after AD treatment at both protein and mRNA levels (**Figure 2C**, ***P<0.001), indicating that AD may have anti-tumor activities in PANC-1 cells. Next, we used the Mito Tracker and confocal analysis to determine the effect of AD on mitochondrial morphology and quantity in PANC-1 cells. Compared to the control group, mitochondria inAD-treated cells were much shorter and fewer (**Figure 2D**). Analysis of mitochondrial function using JC-1 staining revealed that compared to the control group, AD-treated PANC-1 cells exhibited a red-to-green fluorescence switch for JC-1, as well as considerably lower mitochondrial membrane potential (**Figure 2E**, **2F**, ***P<0.001), indicating that suppression of PANC-1 cell growth by AD is associated with mitochondrial dysfunction.

Identification of PTPMT1 interactors by mass spectrometry

Due to the lack of a commercially available anti-PTPMT1 antibody for IP, we constructed a lentiviral overexpression vector encoding Flag-tagged PTPMT1 and carried out co-immunoprecipitation (co-IP) to capture PTPMT1 interactors. We identified 10,871 potential interactors using mass spectrometry (**Figure 3A**). Next, we subjected these candidate interactors to GO and KEGG pathway analysis using DAVID and identified the top 6 terms regulated by PTPMT1 in biological process, Reactome, molecular function, as well as KEGG pathway as shown in **Figure 3B-E**. These results indicate that potential PTPMT1 interactions are tightly associated with mitochondrial function. Based on the number of unique peptides, 10 target genes were selected for further experimental validation.

Verification of PTPMT1 interacting proteins using co-immunoprecipitation

Using bioinformatics analysis of proteins most likely to interact with PTPMT1, we selected NDUFS2 (NADH: ubiquinone oxidoreductase core subunit S2) and SLC25A6 (Solute Carrier Family 25 Member 6) for validation. To verify the mass spectrometry results, we performed western blotting to detect the presence of NDUFS2 and SLC25A6 following co-IP. This analysis confirmed the presence of both NDUFS2 and SLC25A6 in the protein samples after Flag-PTPMT1 magnetic bead IP (**Figure 4A**). PTPMT1-SLC25A6 interaction was analyzed by immunoprecipitation with IgG or an anti-SLC25A6 antibody in PANC-1 cells (**Figure 4B**). Next, we confirmed the interaction between PTPMT1 and NDUFS2 by reciprocal co-IP (**Figure 4C**). Similar analysis using cells transfected with control or PTPMT1 siRNAs showed that the levels of NDUFS2 and SLC25A6 were dramatically lower in PTPMT1-silenced samples (**Figure 4D**, **4E**,

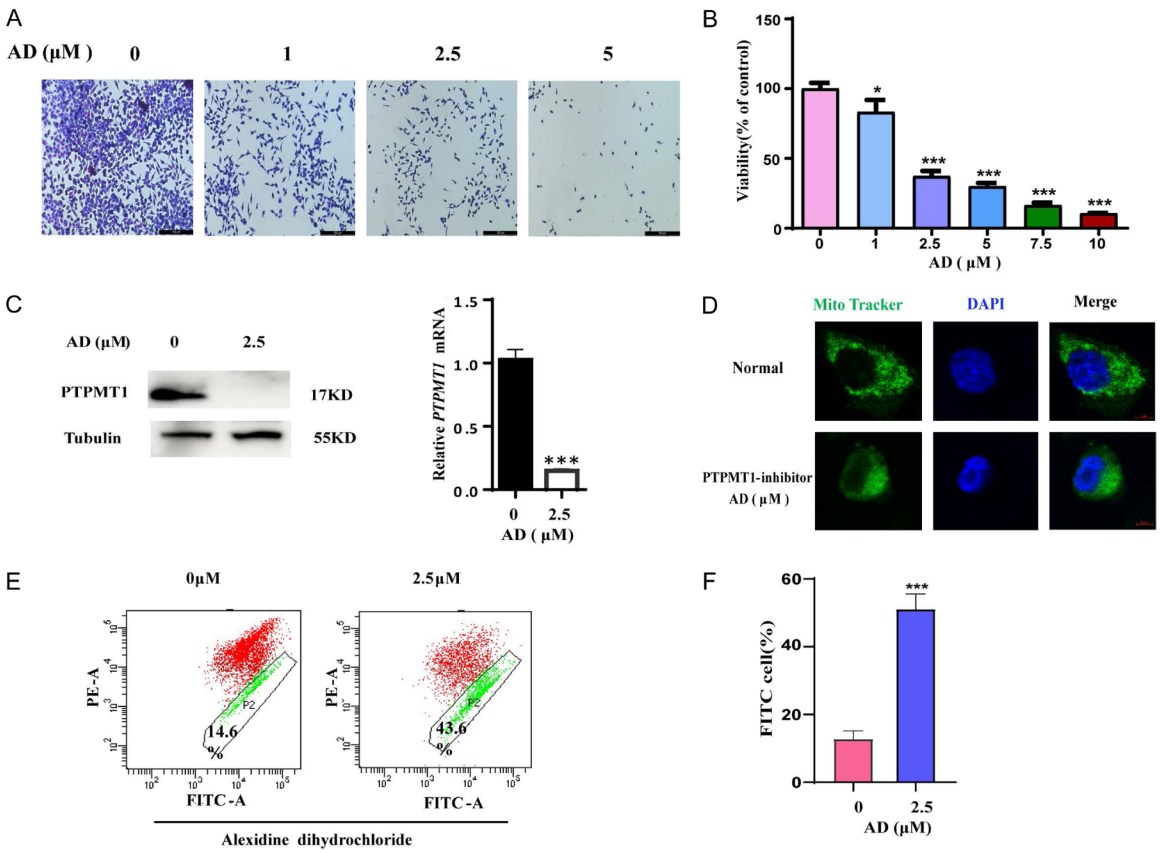

Figure 2. The PTPMT1 inhibitor Alexidine dihydrochloride hinders the viability of PANC-1 cells and promotes apoptosis. (A) Colony formation in PANC-1 cells treated at the indicated concentrations of Alexidine dihydrochloride (AD) (Scale bar: 500 μm; Magnification: 40 ×). (B) CCK8 analysis of the viability of PANC-1 cells incubated with AD. (C) PANC-1 cells were treated with AD for 48 hours. Analysis of protein levels via western blotting (left) and mRNA levels by RT-qPCR (right). (D) PANC-1 cells were incubated with AD for 48 hours and mitochondrial morphology was assessed via confocal microscopy (Scale bar: 10 μm; Magnification: 600 ×). (E) PANC-1 cells were treated with AD for 48 hours and mitochondrial damage was detected by FACS. (F) Quantification of mitochondrial damaged cells (E). Data are given as mean ± SD of three independent experiments (B, C, F), *P<0.05, **P<0.01, ***P<0.001 (two-tailed t-test, B, C, F). Tubulin (B): loading control. Data represent at least two independent experiments (A, C-E).

***P<0.001) at both protein and mRNA levels, and that NDUFS2 levels in SLC25A6-depleted samples were also reduced (**Figure 4F**, **4G**). We did not find any significant change in the levels of PTPMT1 and SLC25A6 in NDUFS2-depleted samples (**Figure 4H**), further confirming the relationship between PTPMT1, NDUFS2, and SLC25A6.

Immunohistochemical staining and gene correlation analysis in pancreatic cancer tissues versus normal adjacent tissues

Next, we performed immunohistochemical staining to examine the expression of PTPMT1, NDUFS2, and SLC25A6 in pancreatic cancer versus paracancerous tissues (**Figure 5A**) and observed that the expression of PTPMT1, NDUFS2, and SLC25A6 were much higher in pancreatic cancer tissues relative to adjacent normal tissues (**Figure 5B-D**, *P<0.05, ***P< 0.001). Bioinformatic analysis confirmed PTPMT1 correlation with NDUFS2 and SLC25A6 (**Figure 5E**, **5F**).

Discussion

Previously, we have reported that PTPMT1 is highly expressed in pancreatic cancer and that its overexpression protects pancreatic cancer from Erastin-induced ferroptosis through regulation of SLC7A11 and ACSL4 [15]. Here, we demonstrated that PTPMT1 silencing or inhibition in PANC-1 and MIA-PACA-II cells could significantly suppress cell viability, cell growth, and colony formation. Moreover, JC-1 staining,

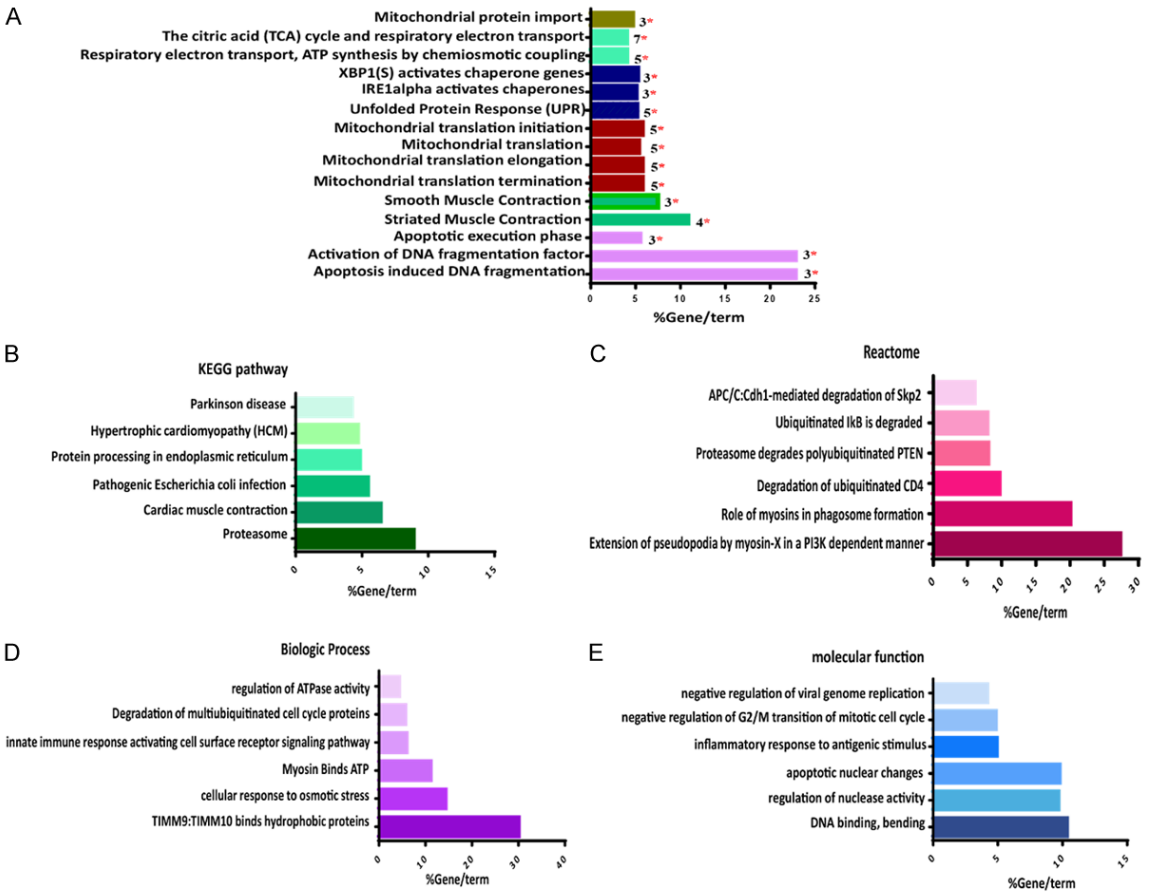

F

Gene	Description	Coverage	Peptides	PSMs	Unique Peptides
SLC25A6	ADP/ATP translocase 3 [Homo sapiens]	24.4966443	20	24	20
NDUFS2	NADH dehydrogenase [ubiquinone] iron-sulfur protein 2, mitochondrial isoform 1 precursor [Homo sapiens]	27.3753528	7	17	7
MYO1C	unconventional myosin-Ic isoform a [Homo sapiens]	23.3480176	7	15	3
COX2	cytochrome c oxidase subunit II [Homo sapiens]	7.55939525	7	9	7
NOC4L	nucleolar complex protein 4 homolog [Homo sapiens]	10.8527132	4	4	4
TIMM50	mitochondrial import inner membrane translocase subunit TIM50 [Homo sapiens]	18.8596491	4	5	3
PSMD7	26S proteasome non-ATPase regulatory subunit 7 [Homo sapiens]	17.9012346	3	3	3
DBN1	drebrin isoform a [Homo sapiens]	17.257319	3	4	3
BANF1	barrier-to-autointegration factor [Homo sapiens]	40.4494382	2	3	2
SNAP23	synaptosomal-associated protein 23 isoform SNAP23A [Homo sapiens]	13.2701422	2	3	2

Figure 3. Identification of PTPMT1-interacting proteins via mass spectrometry. A. A total of 10,871 PTPMT1-interacting proteins were identified by mass spectrometry. B-E. Enriched terms after GO, KEGG pathway, Reactome analyses on DAVID are shown. F. A list of candidate PTPMT1-interacting proteins for further validation.

FACS analysis, and confocal data revealed that PTPMT1 knockdown or inhibition with Alexidine hydrochloride caused mitochondrial damage and impaired its function in PANC-1 and MIA-PACA-II cells. These results indicate that PTPMT1 can modulate mitochondrial respiration and its downregulation promotes the death of PANC-1 and MIA-PACA-II cells.

Mitochondria produce the bulk of the ATP needed by eukaryotic cells. The mitochondrial ADP/ATP carrier (adenine nucleotide carrier/ANCP/ANC) is a nuclear-encoded protein that catalyzes the exchange of mitochondrial ATP synthase-generated ATP4 with cytoplasmically produced ADP3 in most energy-consuming processes. ANCP is a ubiquitous mitochondrial protein that

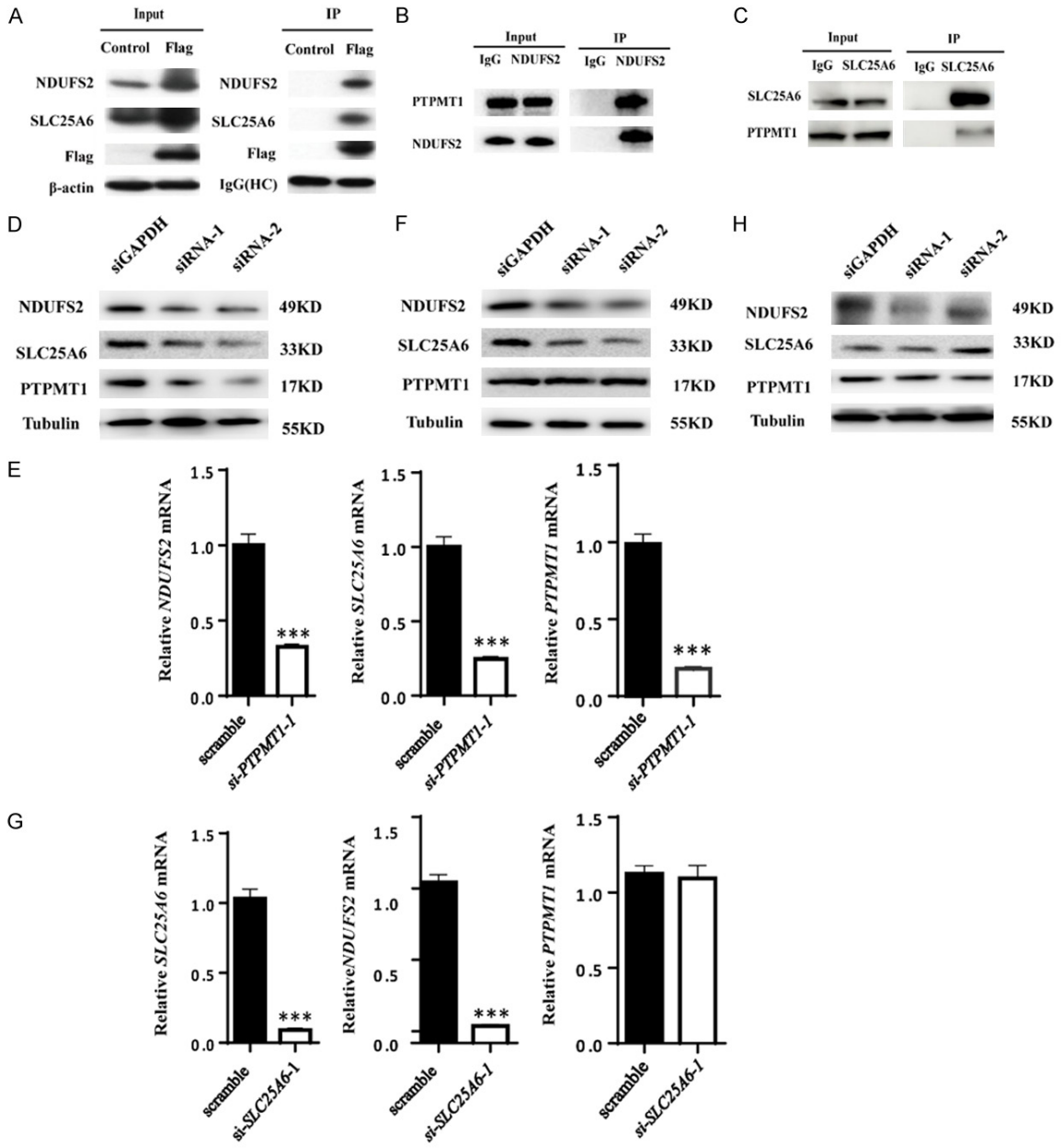

Figure 4. Identification of PTPMT1-interacting proteins by co-immunoprecipitation. (A) The interaction of PTPMT1, NDUFS2, and SLC25A6 was analyzed via immuno-precipitation using anti-Flag beads in Flag-PTPMT1-overexpressing PANC-1 cells. (B) Immunoprecipitation analysis of endogenous interaction between PTPMT1 and SLC25A6 using anti-IgG or anti-SLC25A6 antibodies. (C) Immunoprecipitation analysis of endogenous interaction between PTPMT1 and NDUFS2 using anti-IgG or anti-NDUFS2 antibodies. (D) Protein levels of NDUFS2, SLC25A6, PTPMT1, and tubulin in PTPMT1-silenced and scramble-transfected PANC-1 cells. (E) mRNA levels (RT-qPCR) of NDUFS2, SLC25A6, and PTPMT1 in PTPMT1-silenced and scramble-transfected PANC-1 cells. (F) Protein levels of the indicated proteins in SLC25A6-silenced and scramble-transfected PANC-1 cells. (G) mRNA levels (RT-qPCR) of the indicated proteins in SLC25A6-silenced and scramble-transfected PANC-1 cells. (H) Protein levels of the indicated proteins in NDUFS2-silenced and scramble-transfected PANC-1 cells. Data are given as mean ± SD of three independent experiments (E, G). ***P<0.001, two-tailed t-test (E, G). Tubulin (D, F, H): loading control. Data represent at least two independent experiments (A-D, F, H).

is encoded by four distinct genes: SLC25A4 (ANC1/ANT1), SLC25A6 (ANC2/ANT3), SLC25A5 (ANC3/ANT2), as well as SLC25A31 (ANC4/ANT4) [17]. SLC25A6 is located on the inner membrane of the mitochondria and involved in the exchange of ADP and ATP between the cyto-

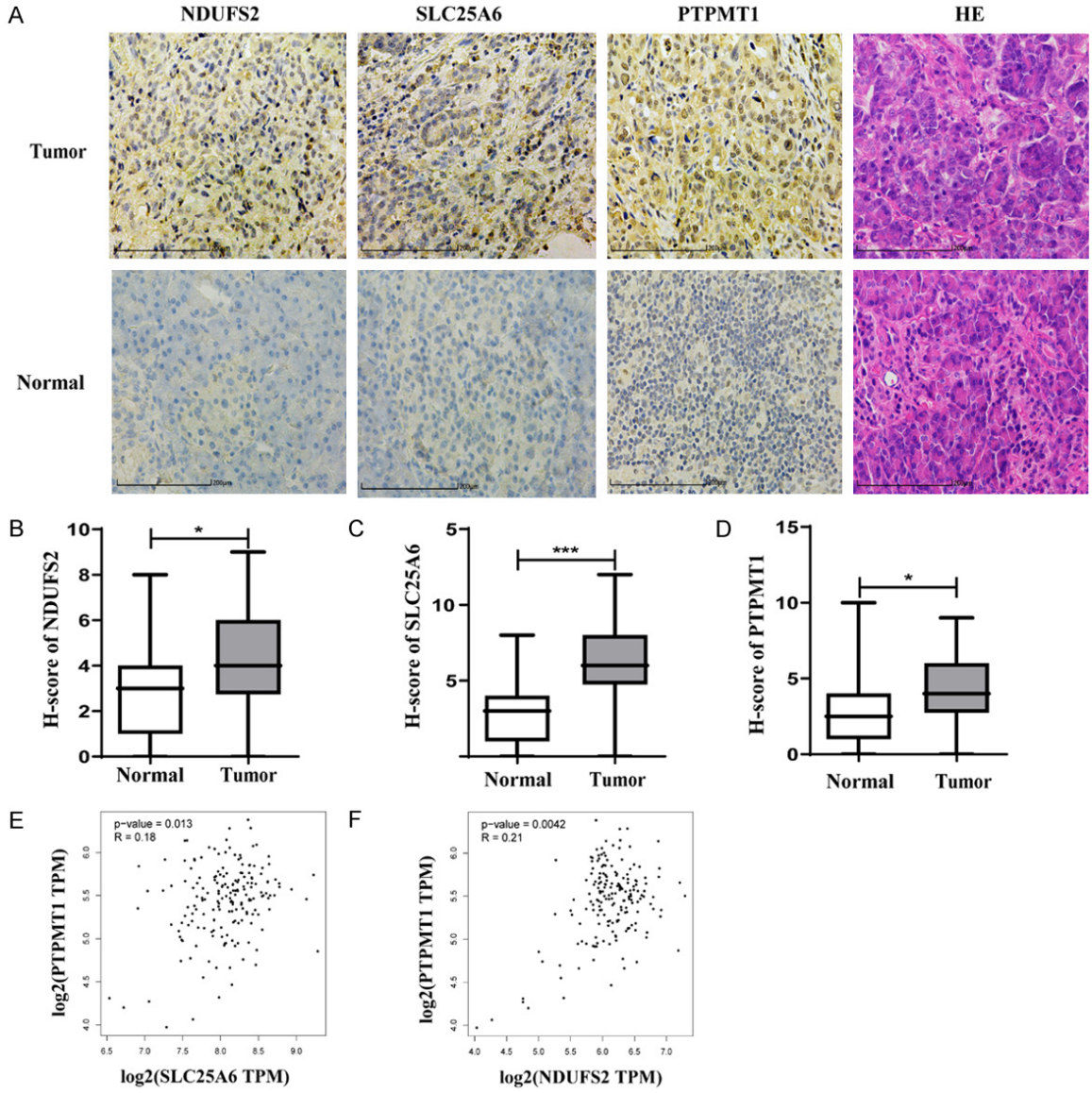

Figure 5. Immunohistochemistry staining and gene correlation analysis in pancreatic cancer tissues versus and adjacent non-tumor tissues. (A) Representative IHC staining of PTPMT1, SLC25A6, and NDUSF2 in PDAC and matched non-tumorous tissues. (Scale bar: 200 μm; Magnification: 40 ×) (B) IHC scores of NDUFS2 expression in PDAC and paired non-tumorous tissues. (C) IHC scores of SLC25A6 expression in PDAC and paired normal tissue. (D) IHC scores of PTPMT1 expression in PDAC and matched non-tumorous tissues. (E) Analysis of correlation between PTPMT1 and SLC25A6. (F) Analysis of correlation between PTPMT1 and NDUFS2. Data are given as mean ± SD. *P<0.05, ***P<0.001 (two-tailed t-test, B-D).

solic and mitochondrial matrix sides [18]. Additionally, ANT is a critical component of the mitochondrial permeability transition pore (MPTP), which is important in the apoptotic process [19, 20] where ANT1 and ANT3 strongly induce apoptosis [15, 21, 22]. A recent study confirmed that Camptothecin could downregulate SLC25A6 and induce apoptosis in a mitochondria-dependent pathway [23]. SLC25A6 isoforms are expressed in all tissues and in cultured fibroblasts at levels that depend on the state of oxidative metabolism [24]. The current work demonstrates that the expression of SLC25A6 increases in cervical carcinoma and precancerous lesion groups, closely linked to HPV status and the carcinogenic protein E6/E7 [25]. Here, we find that PTPMT1 knockdown correlates with reduced SLC25A6 expression

and that SLC25A6 expression was more elevated in pancreatic cancer tissues than in adjacent normal tissues.

NDUFS2 is a fundamental component of the mitochondrial respiratory chain complex I (NADH dehydrogenase), which is responsible for transferring electrons from NADH to the respiratory chain [26, 27]. ATP production and neural stem cell proliferation were both severely reduced in a conditional knockout mouse model with lowered NDUFS2 expression in radial glial and neural stem cells [28]. Perinatal brain development in these mice was also severely hampered, and the mice perished before postnatal day 10. Mutations affecting NCUM, *Yarrowia lipolytica's* homolog of human NDUFS2, caused a complete absence of complex I expression as well as a moderate reduction in Complex I activity [29]. CRISPR/Cas9-mediated NDUFS2 mutation in HEK293 cells for 72 hours remarkably elevated ROS production [30]. Excessive ROS levels can facilitate cell damage and even death [31]. The mutant displayed that increased NDUFS2 mutations also increased apoptosis and necrosis. Interfering with intracellular NDUFS2 levels can hamper the activity of the mitochondrial respiratory chain complex I, reduce intracellular ATP production, inhibit tumor growth, and drastically reduce cancer metastasis [32]. These effects are similar to those of PTPMT1 during tumorigenesis.

To elucidate further the mechanism through which PTPMT1 protects cells from mitochondria death in PANC-1 cells, we examined the interaction of PTPMT1 with SLC25A6 and NDUFS2 using co-immunoprecipitation. Furthermore, when we silenced PTPMT1 or SLC25A6, NDUFS2 expression was downregulated, while PTPMT1 silencing resulted in the downregulation of both SLC25A6 and NDUFS2. In comparison, there was no significant change in the expression of PTPMT1 or SLC25A6 with NDUFS2 silencing. These results indicate that PTPMT1 may regulate the integrity and function of mitochondria, and modulate cell metabolism and death via the SLC25A6-NDUFS2 axis. PTPMT1 may regulate the activity and location of the transcription factors of NDUFS2 and SLC25A6 to impact their expression, although the detailed mechanisms need to be further explored in future studies. Further investigations should explore the role of PTPMT1 in pancreatic cancer tumorigenesis *in vivo* using animal models.

Conclusion

Here, we show that PTPMT1 is upregulated in pancreatic ductal adenocarcinoma and that it possesses a key role in cell proliferation and mitochondrial function by regulating the SLC25A6-NDUFS2 axis. The important physiological mechanism by which PTPMT1 protects mitochondrial function is revealed and the results also highlight PTPTM1 as a potential therapeutic target for promoting pancreatic cancer cell death.

Acknowledgements

This research work was funded by the Beijing Shijitan Hospital Youth Foundation (Grant No. 2021 q16).

Disclosure of conflict of interest

None.

Address correspondence to: Hong Liu, Department of Gastroenterology, Beijing Shijitan Hospital of Capital Medical University, No. 10 Tieyi Road, Haidian District, Beijing 100038, P. R. China. E-mail: liuhong_sjt@ccmu.edu.cn; Dr. Dong-Dong Lin, Department of General Surgery, Xuanwu Hospital Capital Medical University, Beijing 100053, P. R. China. E-mail: ldd1231@126.com; Feng-Jun Xiao, Department of Experimental Hematology and Biochemistry, Beijing Institute of Radiation Medicine, Beijing 100850, P. R. China. E-mail: xiaofjun@sina.com

References

[1] Advancing on pancreatic cancer. Nat Rev Gastroenterol Hepatol 2021; 18: 447.

[2] Jain T and Dudeja V. The war against pancreatic cancer in 2020-advances on all fronts. Nat Rev Gastroenterol Hepatol 2021; 18: 99-100.

[3] Pagliarini DJ, Worby CA and Dixon JE. A PTEN-like phosphatase with a novel substrate specificity. J Biol Chem 2004; 279: 38590-38596.

[4] Zhang J, Guan Z, Murphy AN, Wiley SE, Perkins GA, Worby CA, Engel JL, Heacock P, Nguyen OK, Wang JH, Raetz CR, Dowhan W and Dixon JE. Mitochondrial phosphatase PTPMT1 is essential for cardiolipin biosynthesis. Cell Metab 2011; 13: 690-700.

[5] Xiao J, Engel JL, Zhang J, Chen MJ, Manning G and Dixon JE. Structural and functional analy-

sis of PTPMT1, a phosphatase required for cardiolipin synthesis. Proc Natl Acad Sci U S A 2011; 108: 11860-11865.
[6] Pagliarini DJ, Wiley SE, Kimple ME, Dixon JR, Kelly P, Worby CA, Casey PJ and Dixon JE. Involvement of a mitochondrial phosphatase in the regulation of ATP production and insulin secretion in pancreatic beta cells. Mol Cell 2005; 19: 197-207.
[7] Shen J, Liu X, Yu WM, Liu J, Nibbelink MG, Guo C, Finkel T and Qu CK. A critical role of mitochondrial phosphatase Ptpmt1 in embryogenesis reveals a mitochondrial metabolic stress-induced differentiation checkpoint in embryonic stem cells. Mol Cell Biol 2011; 31: 4902-4916.
[8] Yu WM, Liu X, Shen J, Jovanovic O, Pohl EE, Gerson SL, Finkel T, Broxmeyer HE and Qu CK. Metabolic regulation by the mitochondrial phosphatase PTPMT1 is required for hematopoietic stem cell differentiation. Cell Stem Cell 2013; 12: 62-74.
[9] Sheng J, Zhao Q, Zhao J, Zhang W, Sun Y, Qin P, Lv Y, Bai L, Yang Q, Chen L, Qi Y, Zhang G, Zhang L, Gu C, Deng X, Liu H, Meng S, Gu H, Liu Q, Coulson JM, Li X, Sun B and Wang Y. SRSF1 modulates PTPMT1 alternative splicing to regulate lung cancer cell radioresistance. EBioMedicine 2018; 38: 113-126.
[10] Park H, Kim SY, Kyung A, Yoon TS, Ryu SE and Jeong DG. Structure-based virtual screening approach to the discovery of novel PTPMT1 phosphatase inhibitors. Bioorg Med Chem Lett 2012; 22: 1271-1275.
[11] Bao MH, Yang C, Tse AP, Wei L, Lee D, Zhang MS, Goh CC, Chiu DK, Yuen VW, Law CT, Chin WC, Chui NN, Wong BP, Chan CY, Ng IO, Chung CY, Wong CM and Wong CC. Genome-wide CRISPR-Cas9 knockout library screening identified PTPMT1 in cardiolipin synthesis is crucial to survival in hypoxia in liver cancer. Cell Rep 2021; 34: 108676.
[12] Niemi NM, Lanning NJ, Westrate LM and MacKeigan JP. Downregulation of the mitochondrial phosphatase PTPMT1 is sufficient to promote cancer cell death. PLoS One 2013; 8: e53803.
[13] Xu QQ, Xiao FJ, Sun HY, Shi XF, Wang H, Yang YF, Li YX, Wang LS and Ge RL. Ptpmt1 induced by HIF-2alpha regulates the proliferation and glucose metabolism in erythroleukemia cells. Biochem Biophys Res Commun 2016; 471: 459-465.
[14] Huang XD, Xiao FJ, Guo YT, Sun Y, Zhang YK and Shi XJ. Protein tyrosine phosphatase 1 protects human pancreatic cancer from erastin-induced ferroptosis. Asian J Surg 2022; 45: 2214-2223.
[15] Bauer MK, Schubert A, Rocks O and Grimm S. Adenine nucleotide translocase-1, a component of the permeability transition pore, can dominantly induce apoptosis. J Cell Biol 1999; 147: 1493-1502.
[16] Doughty-Shenton D, Joseph JD, Zhang J, Pagliarini DJ, Kim Y, Lu D, Dixon JE and Casey PJ. Pharmacological targeting of the mitochondrial phosphatase PTPMT1. J Pharmacol Exp Ther 2010; 333: 584-592.
[17] Silva-Marrero JI, Saez A, Caballero-Solares A, Viegas I, Almajano MP, Fernandez F, Baanante IV and Meton I. A transcriptomic approach to study the effect of long-term starvation and diet composition on the expression of mitochondrial oxidative phosphorylation genes in gilthead sea bream (Sparus aurata). BMC Genomics 2017; 18: 768.
[18] Klingenberg M. Molecular aspects of the adenine nucleotide carrier from mitochondria. Arch Biochem Biophys 1989; 270: 1-14.
[19] Petit PX, Lecoeur H, Zorn E, Dauguet C, Mignotte B and Gougeon ML. Alterations in mitochondrial structure and function are early events of dexamethasone-induced thymocyte apoptosis. J Cell Biol 1995; 130: 157-167.
[20] De Giorgi F, Lartigue L, Bauer MK, Schubert A, Grimm S, Hanson GT, Remington SJ, Youle RJ and Ichas F. The permeability transition pore signals apoptosis by directing Bax translocation and multimerization. FASEB J 2002; 16: 607-609.
[21] Zamora M, Granell M, Mampel T and Vinas O. Adenine nucleotide translocase 3 (ANT3) overexpression induces apoptosis in cultured cells. FEBS Lett 2004; 563: 155-160.
[22] Yang Z, Cheng W, Hong L, Chen W, Wang Y, Lin S, Han J, Zhou H and Gu J. Adenine nucleotide (ADP/ATP) translocase 3 participates in the tumor necrosis factor induced apoptosis of MCF-7 cells. Mol Biol Cell 2007; 18: 4681-4689.
[23] Hu Z, Guo X, Yu Q, Qiu L, Li J, Ying K, Guo C and Zhang J. Down-regulation of adenine nucleotide translocase 3 and its role in camptothecin-induced apoptosis in human hepatoma QGY7703 cells. FEBS Lett 2009; 583: 383-388.
[24] Stepien G, Torroni A, Chung AB, Hodge JA and Wallace DC. Differential expression of adenine nucleotide translocator isoforms in mammalian tissues and during muscle cell differentiation. J Biol Chem 1992; 267: 14592-14597.
[25] Hao Y, Ye M, Chen X, Zhao H, Hasim A and Guo X. Discovery and validation of FBLN1 and ANT3 as potential biomarkers for early detection of cervical cancer. Cancer Cell Int 2021; 21: 125.
[26] Fernandez-Aguera MC, Gao L, Gonzalez-Rodriguez P, Pintado CO, Arias-Mayenco I, Garcia-Flores P, Garcia-Perganeda A, Pascual

A, Ortega-Saenz P and Lopez-Barneo J. Oxygen sensing by arterial chemoreceptors depends on mitochondrial complex I signaling. Cell Metab 2015; 22: 825-837.

[27] Wolin MS, Alruwaili N and Kandhi S. Studies on hypoxic pulmonary vasoconstriction detect a novel role for the mitochondrial complex I subunit Ndufs2 in controlling peroxide generation for oxygen-sensing. Circ Res 2019; 124: 1683-1685.

[28] Cabello-Rivera D, Sarmiento-Soto H, Lopez-Barneo J and Munoz-Cabello AM. Mitochondrial complex I function is essential for neural stem/progenitor cells proliferation and differentiation. Front Neurosci 2019; 13: 664.

[29] Gerber S, Ding MG, Gerard X, Zwicker K, Zanlonghi X, Rio M, Serre V, Hanein S, Munnich A, Rotig A, Bianchi L, Amati-Bonneau P, Elpeleg O, Kaplan J, Brandt U and Rozet JM. Compound heterozygosity for severe and hypomorphic NDUFS2 mutations cause non-syndromic LHON-like optic neuropathy. J Med Genet 2017; 54: 346-356.

[30] Bandara AB, Drake JC, James CC, Smyth JW and Brown DA. Complex I protein NDUFS2 is vital for growth, ROS generation, membrane integrity, apoptosis, and mitochondrial energetics. Mitochondrion 2021; 58: 160-168.

[31] Wittmann C, Chockley P, Singh SK, Pase L, Lieschke GJ and Grabher C. Hydrogen peroxide in inflammation: messenger, guide, and assassin. Adv Hematol 2012; 2012: 541471.

[32] Liu L, Qi L, Knifley T, Piecoro DW, Rychahou P, Liu J, Mitov MI, Martin J, Wang C, Wu J, Weiss HL, Butterfield DA, Evers BM, O'Connor KL and Chen M. S100A4 alters metabolism and promotes invasion of lung cancer cells by up-regulating mitochondrial complex I protein NDUFS2. J Biol Chem 2019; 294: 7516-7527.

Supplementary Table 1. The primer sequences for different genes

Gene	Forward primer	Reverse primer
β-actin	Forward 5'GACATGCCGCCTGGAGAAAC3'	Reverse 5'AGCCCAGGATGCCCTTTAGT3'
PTPMT1	Forward 5'TTCTACCCGACGCTCCTA3'	Reverse 5'TTCTACCCGACGCTGCTCTA3'
SLC25A6	Forward 5'GCAACCTTGCCAACGTCATTC3'	Reverse 5'CCGCAAAGTACCTCCAGAACT3'
NDUFS2	Forward 5'GTCCGATTGCCGATTCAGC3'	Reverse 5'GCTTGGGTACATAACAGCTCC3'

Supplementary Table 2. The siRNA sequences targeting different genes

Gene	Forward Primer	Reverse Primer
NDUFS2 (siRNA-1)	Forward 5'GCAGAUGUCGUUGCCAUCAUATT3'	Reverse 5'UAUGAUGGCAACGACAUCUGCIT3'
NDUFS2 (siRNA-2)	Forward 5'GCUGUUAUGUACCCAAGCAAATT3'	Reverse 5'UUUGCUUGGGUACAUAACAGCTT3'
PTPMT (siRNA-1)	Forward 5'GCUGGAUGUUCOUAAAGAGUUTT3'	Reverse 5'AACUCUUUAAGAACAUCCAGCTT3'
PTPMT1 (siRNA-2)	Forward 5'GUGUGUUUACGUGCAUUGUAATT3'	Reverse 5'UUACAAUGCACGUAAACACACTT3'
SLC25A6 (siRNA-1)	Forward 5'CGUCGACUGUUGGAGGAAGAUTT3'	Reverse 5'AUCUUCCUCCAACAGUCGACGTT3'
SLC25A6 (siRNA-2)	Forward 5'CGUGGACUGCAUUGUCCGCAUTT3'	Reverse 5'AUGCGGACAAUGCAGUCCACGTT3'
GAPDH	Forward 5'GUAUGACAACAGCCUCAAGTT3'	Reverse 5'CUUGAGGCUGUUGUCAUACTT3'